Kinetic Investigations on the Redox Reactions of Platinum Carbonyl Clusters with Dihydrogen and Acid

Sumit Bhaduri,*,† Goutam Kumar Lahiri,*,‡ Doble Mukesh,§ Himadri Paul,‡ and Krishna Sarma†

Reliance Industries Limited, Swastik Mills Compound, V.N. Purav Marg, Chembur, Mumbai-400 071, India, and Department of Chemistry, Indian Institute of Technology, Powai, Mumbai 400 076, India, and John F Welch Technology Center (GEITC Pvt. Ltd.), Whitefield Road, Bangalore 560066, India

Received March 21, 2001

Redox reactions of the Chini clusters, $[Pt_3(CO)_6]_n^{2-}$ ($n = 3, 4, 5$), with dihydrogen and acid have been kinetically studied. The reduction of the tetramer to the trimer by dihydrogen is found to be second order with respect to the cluster concentration. Within the pressure range of 1−7 bar, the rate is independent of hydrogen pressure. The acid-induced oxidations of the trimer to the tetramer in DMF and the tetramer to the pentamer in both DMF and acetonitrile proceed through fast protonation equilibria followed by rate-determining steps. The consecutive oxidation of the trimer → tetramer → pentamer can be accurately simulated by assuming a three rate constant kinetic model. While the oxidation of the trimer involves more than one protonation equilibria between the free cluster and the protonated species, for the tetramer there is one equilibrium with a 1:1 cluster to proton molar ratio. Cyclic voltammetric studies on the trimer in DMF and the tetramer in acetonitrile show three and two anodic responses in the potential ranges −0.42 to −0.08 and 0.4 to 0.75 V, respectively. The kinetic findings and literature-reported spectroscopic and other observations are consistent with a mechanism that involves the formation of weak aggregates of the clusters and disproportionation of the aggregates.

Introduction

Exploring the connections between clusters and colloids is an important current theme of chemical research.[1] In terms of reactivity meaningful comparisons between clusters and colloids require identification and investigation of reactions that are unique to these classes of substances.

The platinum clusters of general formula $[Pt_3(CO)_6]_n^{2-}$ (n = 1−6, ∼10), known as Chini clusters, exhibit intriguing molecular architecture, dynamic NMR behavior, and spectral signatures.[2−4] As shown by equilibrium (a) in Scheme 1, the Chini clusters can equilibrate two protons and two electrons with dihydrogen. We had explored[5] the catalytic potential of this reaction and have recently shown[6] that in the presence of the platinum clusters, the dye methyl viologen (MV^{2+}) is reduced by dihydrogen to the methyl viologen radical cation ($MV^{\bullet+}$).

In systems designed for the solar photoreduction of water, metal colloids in general and platinum colloids in particular bring about reactions that are strikingly similar to the above-mentioned reactions of the clusters.[7] In these systems $MV^{\bullet+}$, often used as the photochemical mediator, reacts with protons at the metal colloid to produce dihydrogen. The production of dihydrogen is thought to involve reactions (b) and (c). The similarities between (a) and (c) are obvious. While the kinetics of reactions (b) and (c) have been successfully analyzed by using a microelectrode model, mechanistic information on (a) is not available.[8]

* Corresponding authors. E-mail for S.B.: sumit_bhaduri@ril.com. E-mail for G.K.L.: lahiri@ether.chem.iitb.ernet.in.
† Reliance Industries Limited.
‡ Indian Institute of Technology.
§ John F Welch Technology Center.

(1) (a) Braunstein, P.; Kormann, H.; Meyer-Zaika, W.; Pugin, R.; Schimd, G. *Chem.-Eur. J.* **2000**, *6* (24), 4637. (b) Schimd, G. *Prog. Colloid Polym. Sci.* **1998**, *111*, 52. (c) Hasimoto, T.; Saijo, K.; Harada, M.; Toshima, N. *J. Chem. Phys.* **1998**, *109* (13), 5627. (d) Devenish, R. W.; Goulding, T.; Heaton, B, T.; Whyman, R. *J. Chem. Soc., Dalton Trans.* **1996**, *5*, 673. (e) Schimd, G.; Maihack, V.; Lantermann, F.; Peschel, S. *J. Chem. Soc., Dalton Trans.* **1996**, *5*, 589. (f) Evans, J. *J. Chem. Soc., Dalton Trans.* **1996**, *5*, 555. (g) Schimd, G., Ed. *Clusters and Colloids*; VCH: Weinheim, 1994. (h) Lewis, L. N. *Chem. Rev.* **1993,** *93,* 2693. (i) Schimd, G. *Chem. Rev.* **1992**, *92*, 1709. (j) Teo, B. K.; Zhang, H. *J. Cluster Sci.* **1990**, *1*, 155.

(2) (a) Longoni, G.; Chini, P. *J. Am. Chem. Soc.* **1976**, *98*, 7225. (b) Calabrese, J. C.; Dahl, L. F.; Chini, P.; Longoni, G.; Martinengo, S. *J. Am. Chem. Soc.* **1974**, *96*, 2614.

(3) (a) Brown, C.; Heaton, B. T.; Chini. P.; Fumagalli, A.; Longoni, G. *J. Chem. Soc., Chem. Commun.* **1977**, 309. (b) Brown, C.; Heaton, B. T.; Towl, A. D. C.; Chini, P.; Fumagalli, A.; Longoni, G. *J. Organomet. Chem.* **1979,** *181*, 233.

(4) (a) Underwood, D, J.; Hoffmann, R.; Tatsumi, K.; Nakamura, A.; Yamamoto, Y. *J. Am. Chem. Soc.* **1985,** *107,* 5968. (b) Roginski, R. T.; Shapely, J. R.; Drickamer, H. G.; d'Aniello, M. J., Jr. *Chem. Phys. Lett.* **1987**, *135*, 525. (c) Woolley, R. G. *Chem. Phys. Lett.* **1988**, *143*, 145.

(5) (a) Basu, A.; Bhaduri, S.; Sharma, K. *J. Chem. Soc., Dalton Trans.* **1984**, 2315. (b) Bhaduri, S.; Sharma, K. *J. Chem. Soc., Chem. Commun.* **1992**, 1593. (c) Bhaduri, S.; Sharma, K. *J. Chem. Soc., Chem. Commun.* **1996**, 207.

(6) (a) Bhaduri, S.; Mathur, P.; Payra, P.; Sharma, K. *J. Am. Chem. Soc.* **1998**, *120*, 12127. (b) Bhaduri, S. *Curr. Sci.* **2000**, *78*, 1318.

(7) (a) Bard, A. J. *Science* **1980**, *207*, 139. (b) Toshima, N.; Takahashi, T.; Hirai, H. *J. Macromol. Sci. Chem. A* **1988**, *25*, 669. (c) Lehn, J, M.; Sauvage, J. P. Nouv. *J. Chim.* **1977**, *1*, 449. (d) Kalyansundaram, K.; Kiwi, J.; Gratzel, M. *Helv. Chim. Acta* **1978**, *61*, 2720. (e) Harriman, A. *J. Chem. Soc., Chem. Commun.* **1990**, 24.

10.1021/om0102201 CCC: $20.00
Publication on Web 06/27/2001

Scheme 1

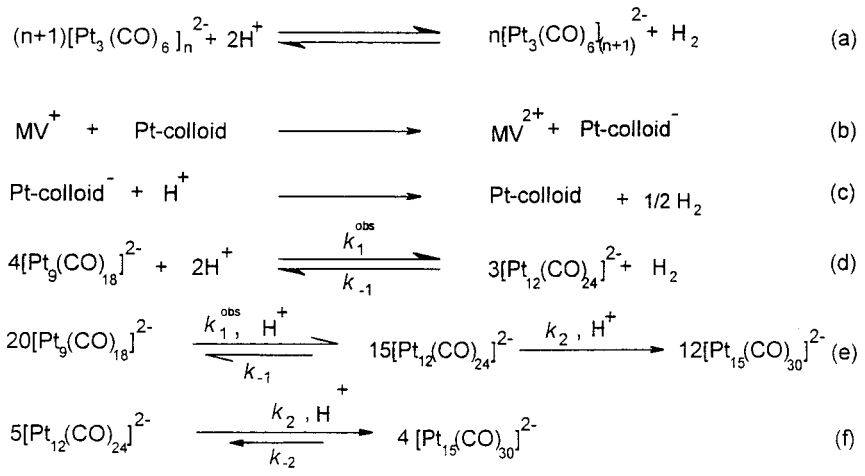

In this paper kinetic results on the forward and backward reaction of equilibrium (d), i.e., equilibrium (a) with $n = 3$, are presented. Kinetic studies on the oxidation of $[Pt_{12}(CO)_{24}]^{2-}$ to $[Pt_{15}(CO)_{30}]^{2-}$ by acid, i.e., the forward reaction of equilibrium (f), are also discussed. Cyclic voltammetric studies on $[Pt_9(CO)_{18}]^{2-}$ and $[Pt_{12}(CO)_{24}]^{2-}$ have been carried out, and these results are discussed. A general mechanistic scheme consistent with the empirical rate laws and the complex molecularities of equilibria (d) and (f) is presented. The proposed mechanism fits well with dynamic NMR (^{195}Pt) data that were reported more than two decades ago.[3]

Results and Discussion

A. General Observations. The platinum carbonyl cluster anions $[Pt_9(CO)_{18}]^{2-}$ (**1**), $[Pt_{12}(CO)_{24}]^{2-}$ (**2**), $[Pt_{15}(CO)_{30}]^{2-}$ (**3**), and $[Pt_{18}(CO)_{36}]^{2-}$ (**4**) have characteristic UV−visible spectra. The reactions depicted by (d) as well as the oxidations of **2** to **3** and **3** to **4** show clean isobesticities (Figure 1). The relative stabilities of **1** to **4** depend on the solvent. In general in the complete absence of agents capable of effecting redox reactions, i.e., protons, hydroxide ions, water, dioxygen, etc., clusters **1** and **2** are stable in *N*,*N*-dimethyl formamide (DMF). Also in DMF under pseudo-first-order conditions both the forward and the backward reactions of equilibrium (d) proceed at convenient rates and could be monitored by spectrophotometry.

However, even by passing a vigorous stream of dihydrogen through an acetontrile solution of **2** for a long time, the formation of **1** could not be observed by spectrophotometry. This behavior is in contrast to the facile reduction of **2** to **1** in DMF. Also, in other solvents such as acetone, tetrahydrofuran, ethyl acetate, and dichloromethane, reduction of **2** by dihydrogen is slow, and at atmospheric pressure of dihydrogen, equilibrium (d) lies mainly to the right. The reduction of **3** to **2** in DMF by dihydrogen is too rapid for rate studies by conventional spectrophotometry and has not been attempted.

Oxidation of the clusters with acid similarly shows a marked dependence on the solvent. As discussed later, in DMF an excess of acid triggers the consecutive oxidation of **1** → **2** → **3**. However, to bring about the complete oxidation of **2** to **3** in DMF, the amount of acid required is at least 2 orders of magnitude higher than that in acetonitrile. In acetonitrile relatively small quantities of acid are required for the oxidation of **2** to **3**, but much larger quantities (∼300 times) are needed to bring about any observable oxidation of **3** to **4**. Furthermore while the oxidation of **3** to **4** in acetonitrile can be brought about by acid, even with excess of acid, such oxidation is not observed in DMF.

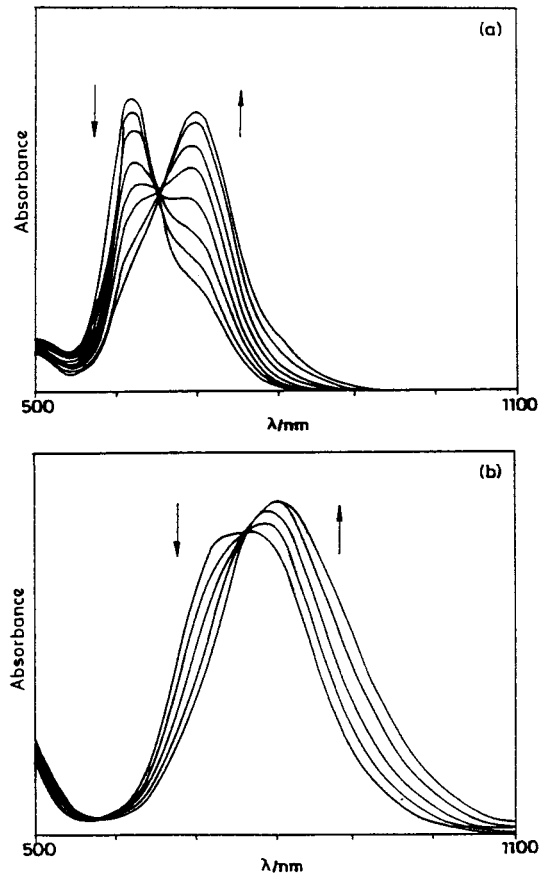

Figure 1. (a) Spectrophotometrically monitored oxidation of **2** to **3** and (b) **3** to **4** by acid in acetonitrile. In (a) 0.2 μM of **2** is reacted with 6 μM HCl; in (b) 0.2 μM of **3** is reacted with 1800 μM HCl. The spectrum with isobesticity for **1** to **2** has been reported earlier.[5]

(8) (a) Miller, D. S.; McLendon, G. *J. Am. Chem. Soc.* **1981**, *103*, 6791. (b) Miller, D. S.; Bard, A. J.; MeLendon, G.; Ferguson, J. *J. Am. Chem. Soc.* **1981**, *103*, 5336.

Taking these considerations into account, the rate studies described below have been carried out in DMF and in one case also in acetonitrile. The kinetic analyses have been performed mainly by simulation methods where the basic strategy is to achieve a good fit between experimental and predicted data points by assuming a *minimum* number of *chemically reasonable* reactions. Each such reaction has an associated rate constant, and the values of these rate constants are optimized to give the best fit. All the reactions taken together are referred to as the kinetic model. Further details of the simulation method are given in the Experimental Section.

B. Reduction of 2 to 1 by Dihydrogen. The order of the backward reaction of equilibrium (d) with respect to the cluster concentration has been studied in DMF. This requires maintenance of dissolved dihydrogen concentration that is much greater than that of **2**. Fortunately in a dihydrogen-saturated DMF solution, because of the high molecular weight of **2** and high solubility of dihydrogen, this condition is easily satisfied.

The reduction of **2** to **1** by dihydrogen is found to be *second order* with respect to the concentration of **2**. Good fits between the simulated concentration profile and the observed data points are obtained only on assuming a second-order rate dependence. This is shown in Figure 2a and has been found to be valid at four different temperatures in the range 300−312 K (Experimental Section). At 300 K the observed rate constant (k_{-1}) is 0.013 ± 0.004 M^{-1} L S^{-1}.

Under elevated pressures of dihydrogen (1 bar $\leq = p(H_2) \leq$ 7 bar) initial rate measurements have also been carried out, and the initial rate has been found to be independent of the applied dihydrogen pressure. In other words within the above-mentioned pressure range, the rate shows zero-order dependence with respect to dihydrogen concentration.

A parity plot (Figure 2b) also validates the above findings. In the parity plot the experimentally determined concentrations of **2** under different conditions (constant temperature but different time intervals with different initial concentrations of **2** and applied dihydrogen pressures) are compared with the predicted ones. The predictions are made by assuming the above-mentioned orders. As can be seen, most of the points are very close to the straight line where the experimental and predicted data coincide.

The temperature dependence of the observed rate constant (k_{-1}) is shown in Figure 5a. It is contrary to Arrhenius type behavior. Instead of a negative slope, a positive slope indicating negative activation energy is observed. The mechanistic significance of this observation is discussed later (section F).

C. Oxidation of 1 to 2 by Protons. Although the oxidation of **1** to **2** by small quantities of acid shows isobesticity, under pseudo-zero-order conditions with respect to acid, i.e., excess acid, complications arise due to further oxidation of **2** to **3**. As shown in Figure 3a, the time-monitored concentration profiles of **1**, **2**, and **3** can be accurately simulated only if a model consisting of the three reactions of (e) (Scheme 1) is assumed. In other words, good fits between experimental data points and simulated concentration profiles require the optimization of three rate constants: k_1^{obs}, k_2, and k_{-1}.

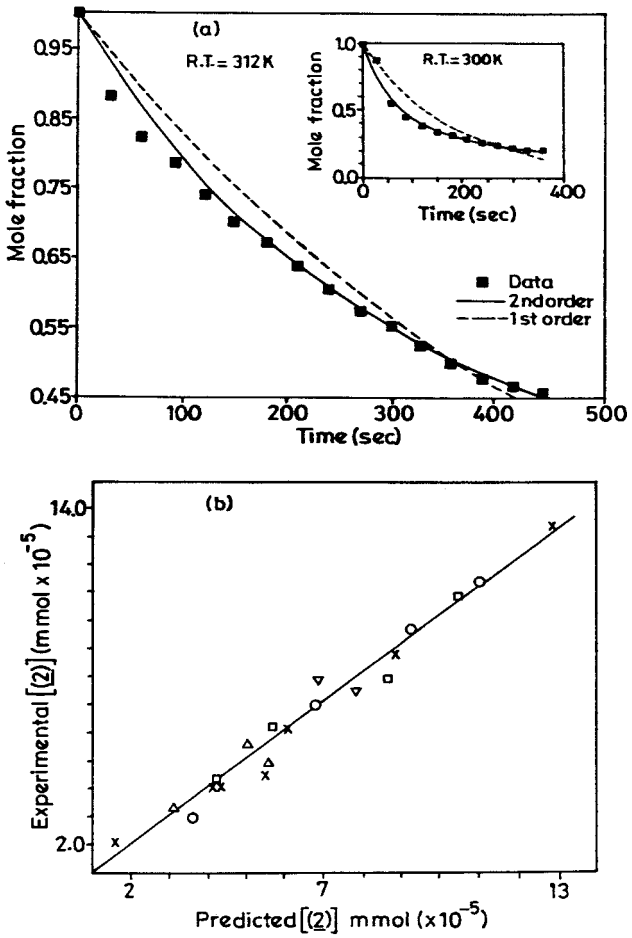

Figure 2. (a) Experimentally determined concentrations of **2** in the reaction of **2** with dihydrogen at 312 K and (inset) 300 K in DMF. The data points are shown by filled squares, and the broken and the solid lines correspond to simulated concentration profiles for first- and second-order reactions respectively with respect to the concentration of **2**. (b) Parity plot, ×, ○, etc., corresponds to data obtained at different hydrogen pressures within 2−7 bar of dihydrogen at 300 K.

As can be seen from Figure 3b, a two rate constant model that ignores the backward reaction, i.e., where k_{-1} is assumed to be zero, gives noticeably poorer fit. As may be expected, because excess acid is used, the accuracy of the simulation is far more sensitive to k_1^{obs} than to the other two rate constants. It may be noted that the simulation technique does not involve any steady-state approximation. In other words the rates of the forward and backward reactions of the first step of (e) are far removed from a situation where they become equal. Thus, although the inclusion of both k_2 and k_{-1} is necessary to improve the fit, their quantification with acceptable standard deviation is achieved only under different experimental conditions. The determination of k_{-1} has already been described in section A and that of k_2 is discussed in section D.

Under pseudo-zero-order conditions with respect to acid, the values of k_1^{obs} have been determined at different acid concentrations. With increasing acid concentrations k_1^{obs} increases, finally reaching a saturation value. Within the acid range $5[(\mathbf{1})] < [H^+] < 25[(\mathbf{1})]$, a plot of $1/k_1^{obs}$ versus $1/[H^+]$ gives a least-squares fitted straight line ($R^2 \approx 0.97$) with a *negative* intercept.

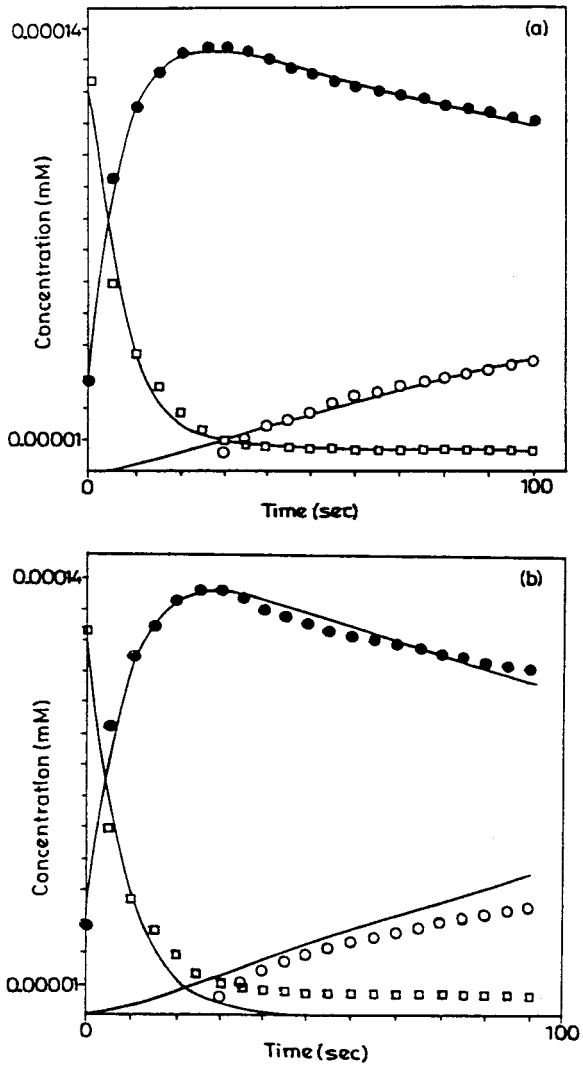

Figure 3. Experimentally determined concentrations of **1**, **2**, and **3** are represented by □, ●, and ○ in the reaction of **1** with acid at 293 K in DMF. Lines are simulated concentration profiles. In (a) the kinetic model uses three rate constants (k_1^{obs}, k_{-1}, and k_2) and in (b) two rate constants (k_1^{obs}, k_2).

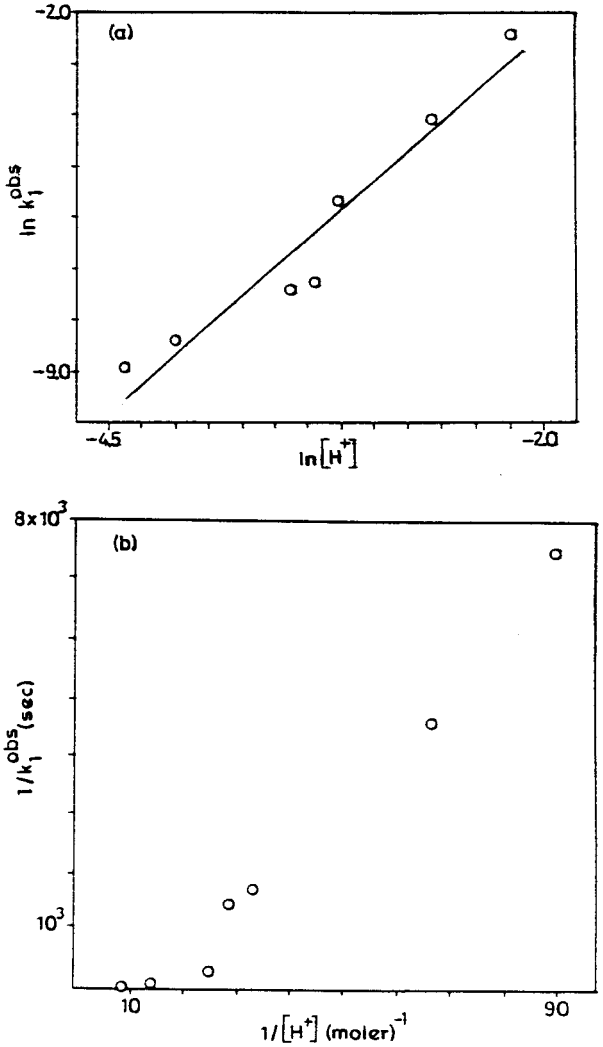

Figure 4. (a) Plot of $\ln(k_1^{obs})$ versus $\ln[H^+]$. (b) Plot of $1/k_1^{obs}$ versus $1/[H^+]$ with same data and intercept set to zero.

A chemically reasonable explanation for the negative intercept is impossible to find. If the intercept is set to zero, departure from linearity ($R^2 \approx 0.88$) is observed (Figure 4b).

A double logarithmic plot of $\ln(k_1^{obs})$ versus $\ln[H^+]$ however gives a straight line ($R^2 \approx 0.93$) with a slope of 2.85 ± 0.35 (Figure 4a). The fact that saturation kinetics is observed means that there is a fast protonation equilibrium followed by the rate-determining step. Since the slope of the double logarithmic plot is nonintegral and between 2 and 3, it may be reasonably assumed that there is more than one equilibrium and the proton to **1** molar ratios in the dominant preequilibria are 2 and 3.

The value of the saturation rate constant k_1^{obs}(290 K) is 0.06 ± 0.01 s^{-1}. It has been measured at four different temperatures and found to be virtually invariant in the temperature range 290−302 K (Figure 5a, inset). This indicates a negligible or zero activation energy barrier. The mechanistic significance of this observation is discussed later (section F).

D. Oxidation of 2 and 3 by Protons. The rate of oxidation of **2** to **3** by protons in acetonitrile and in DMF has been analyzed by the simulation method. Here a two rate constant model as shown by equation (f) is sufficient to give a good fit between the experimental and the predicted data points (Figure 5b). Although inclusion of k_{-2} is necessary for a chemically meaningful model, the accuracy of the simulation is overwhelmingly dependent on k_2 and to a negligible extent on k_{-2}. This obviously is due to the fact that with a large excess of acid (pseudo-zero-order with respect to acid) quantitative contribution of the backward reaction to the observed concentration profile is very little.

In both DMF and acetonitrile, with increasing acid concentration, the observed rate constant (k_2^{obs}) reaches a saturation value. In both the solvents double reciprocal plots of $1/k_2^{obs}$ versus $1/[H^+]$ result in straight lines (Figure 5b, inset). These observations indicate that the rate-determining steps are preceded by fast protonation equilibria and k_2^{obs} is equal to $k_2K[H^+]/(1 + K[H^+])$. As measured from the double reciprocal plots, the rate and equilibrium constants at 300 K in DMF and CH_3CN are $k_2(DMF) = (24 \pm 4) \times 10^{-4}$ s^{-1}, $k_2(CH_3CN) = (91 \pm 5) \times 10^{-4}$ s^{-1}; $K(DMF) = (2.6 \pm 0.4) \times 10^5$ M^{-1}, and $K(CH_3CN) = (5.8 \pm 0.3) \times 10^7$ M^{-1}.

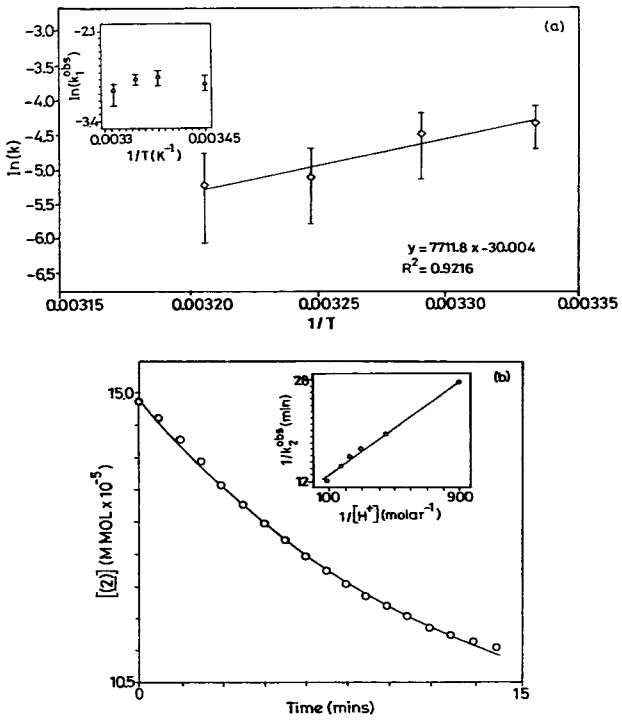

Figure 5. (a) Plot of ln k_{-1} versus $1/T$. Inset: plot of ln k_1^{obs} versus $1/T$. (b) Data points (○) obtained by treating **2**, 0.15 μM, with acid, 3 μM, at 293 K in DMF. The line shows the two rate constant based simulated concentration profile of **2**. (b) Plot of $1/k_2^{obs}$ versus $1/[H^+]$ for data obtained at 293 K in acetonitrile.

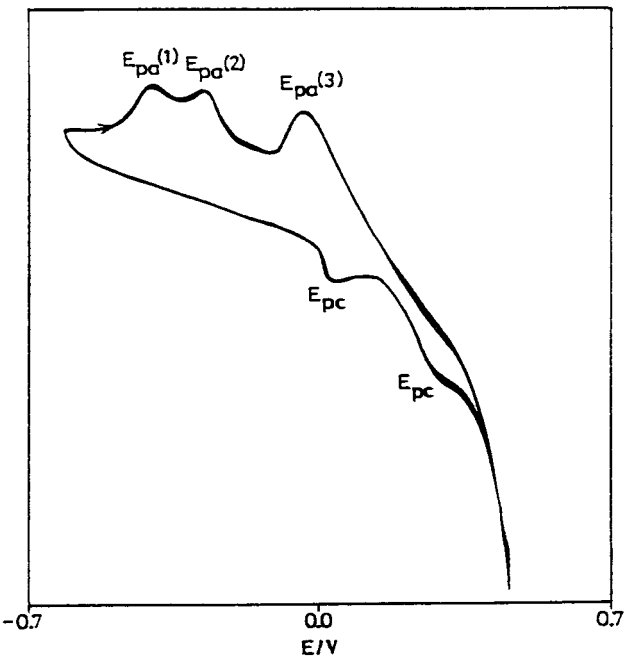

Figure 6. Cyclic voltammogram of the oxidation of **1** in DMF (scan rate: 50 mV s^{-1}).

E. Cyclic Voltammetric Studies. The redox properties of **1** have been examined by cyclic voltammetric technique in DMF solvent using a platinum working electrode. A representative voltammogram is shown in Figure 6. It displays three successive irreversible oxidative responses at $E_{pa}(1)$, −0.42 V ($\Delta G \approx +40$ kcal); $E_{pa}(2)$, −0.3 V ($\Delta G \approx +29$ kcal); and $E_{pa}(3)$, −0.08 V ($\Delta G \approx +8$ kcal) versus SCE. The cyclic voltammetric current heights of the responses are found to be almost identical. The difference in potential between the third and second responses ($E_3 - E_2 = 0.22$ V) is greater than that of the second and first ($E_2 - E_1 = 0.12$ V). The profile and potentials of the voltammograms remain unaltered even after several consecutive scans (Figure 6). On scan reversal it shows two cathodic responses at higher potentials, $E_{pc,}$ 0.23 and 0.01 V.

As already mentioned under ambient conditions the reduction of **2** to **1** by dihydrogen in acetonitrile, to a spectrophotometrically observable extent, cannot be achieved. Due to this reason **2** has been used as the starting material for the cyclic voltammetric studies in acetonitrile. Here two successive irreversible oxidative responses at $E'_{pa}(2)$, 0.4 V ($\Delta G \approx -39$ kcal), and $E'_{pa}(3)$, 0.75 V ($\Delta G \approx -72$ kcal), versus SCE are seen. The cyclic voltammetric current heights of the responses are found to be almost identical to that in the case of DMF, but on scan reversal no cathodic responses are found.

In both the solvents, due to the inherent irreversible nature of the electron-transfer processes, it has not been possible to carry out stepwise spectroelctrochemical study. However, it may be noted that the electrochemical responses are well within the range of other large platinum carbonyl clustures such as $[Pt_a(CO)_b]^{n-}$ (a = 24, 26, and 38; b = 30, 32, and 44, respectively) for which such studies have been reported.[9]

The observed redox processes may be interpreted on the basis of the solution behavior of the clusters. Since cluster **1** is known to undergo acid-induced facile, successive, two-electron oxidations, it is logical to ascribe the three oxidative responses in DMF, $[E_1 - E_3]$, to such oxidations. In other words it is proposed that the three oxidations correspond to **1** → **2**, **2** → **3**, and **3** → **4**. The observed two cathodic responses (E_{pc}) on scan reversal are not easily explained. Presumably the electrogenerated **4** is reduced to some species other than **3**, **2**, or **1**. Similarly in view of the acid-induced oxidation chemistry of **2** in acetonitrile, it is tempting to ascribe the two oxidative responses to **2** → **3** and **3** → **4**. This explanation however invokes a huge solvent effect, which though not easily explained is also indicated by the qualitative observations described in section A.

Assuming that the potential of the $2H^+/H_2$ couple is approximately the same in DMF and acetonitrile, and ignoring the kinetic barriers of the processes, the calculated free energy values are found to be in accordance with most of these observations. Thus probably because of favorable thermodynamics, less acid is required to effect the oxidation of **2** to **3** in acetonitrile than in DMF. Similarly the oxidation of **3** to **4** in DMF is thermodynamically unfavorable and cannot be effected even with a large amount of acid. In acetonitrile it is thermodynamically favorable and can be effected.

F. Proposed Mechanism. Apart from the empirically derived rate expressions, any proposed mechanism should take into account the complex molecularities of equilibria (d) and (f). It is also important to bear in mind that in the reactions of the platinum carbonyls with dihydrogen no intermediates could be seen by NMR. This was reported[2] by Chini and Longoni and confirmed

(9) Roth, J. D.; Lewis, G. J.; Safford, L. K.; Jiang, X.; Dahl, L. F.; Weaver, M. J. *J. Am. Chem. Soc.* **1992**, *114*, 6159.

Scheme 2

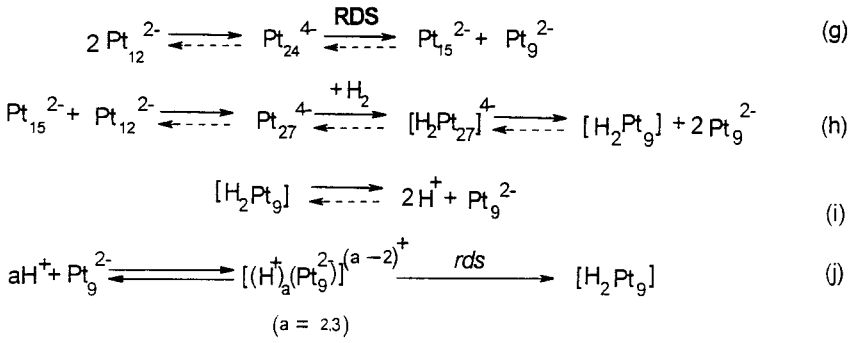

Scheme 3

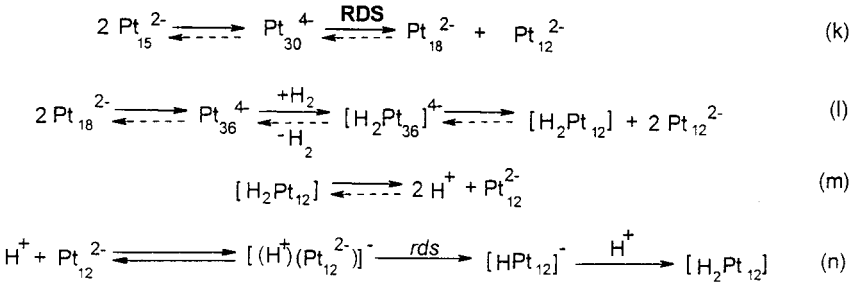

by us. The intermediates are therefore transitory and/or never accumulate in sufficient concentration to be detectable by NMR spectroscopy. This conclusion is also supported by the fact that in the spectrophotometric monitoring of these redox reactions clean isobesticities are observed.

For the reduction of **2** to **1** by dihydrogen, the mechanism shown in Scheme 2 is proposed. The carbonyl groups are omitted for clarity. The mechanism is consistent with the empirically derived rate laws and rationalizes the stoichiometry (d). It also fits in well with previously reported ^{195}Pt NMR studies where in a mixture of **1** and **2** intermolecular exchange of platinum triangles was observed.[3]

In the reduction of **2** to **1** by dihydrogen, the second-order dependence of the rate on the concentration of **2** is indicative of dimerization of **2**. Since the rate law is found to be independent of dihydrogen concentration, the rate-determining step must precede reaction steps involving dihydrogen. The dimerization is therefore proposed to be followed by the rate-determining disproportionation of the dimer to give 1 mol each of **1** and **3**. The amount of **3** produced in this step is proposed to be very small. Consequently it is not detected by spectrophotometry. The dimerization equilibrium and the rate-determining step, marked RDS, are shown by (g) in Scheme 2.

As already mentioned in the reduction of **2** to **1**, the Arrhenius plot gives a straight line with a positive slope. An equilibrium followed by the rate-determining step, as shown by (g), would make the observed rate constant a product of the equilibrium constant of the dimerization step and the rate constant of the disproportionation step. In the Arrhenius plot the observed slope would be equal to $-(\Delta G + \Delta E^{\#})$, where ΔG is the change in free energy associated with the equilibrium. If ΔG were negative and $|\Delta G| > |\Delta E^{\#}|$, a positive slope would result. Such explanations for apparent "negative" activation energy are common, and a recent literature reference is given.[10]

The steps shown by (h) to (i) are fast. Cluster **3** produced in (g) forms an aggregate with **2** to give a trimer of **1**. It is proposed that the trimer of **1** reacts with dihydrogen and accepts two electrons to give 2 mol of **1** and 1 mol of $[H_2Pt_9]$. The latter complex is a tight ion pair of two protons with **1** where the two H^+ are present in the inner coordination sphere of **1**. The cluster $[H_2Pt_9]$ dissociates into two protons and one molecule of **1** in step (i), and the observed stoichiometry of equilibrium (d) is satisfied.

The same mechanism with slight modification is proposed for the oxidation of **1** to **2**. The only additional step shown by (j) is due to the presence of excess acid. As discussed earlier, the rate expression suggests equilibria involving $[H^+]$, **1**, and multiprotonated species. These multiprotonated species, which are proposed to be weak ion pairs, undergo rate-determining conversion, marked *rds*, to the tight ion pair $[H_2Pt_9]$. According to the principle of microscopic reversibility, the conversion of **1** to **2** then proceeds through the backward reactions of (h) and (g), as shown by broken arrows. Here also the observed rate constant is a product of the equilibrium constant for protonation and the true rate constant. If ΔG for the equilibrium were negative and $|\Delta G| = |\Delta E^{\#}|$, the observed activation energy would be zero or near zero.

The reduction of **3** to **2** by dihydrogen is too rapid and has not been studied. However, a very similar mechanism may be proposed for the reduction of **3** to **2** by dihydrogen. This is shown in Scheme 3 (carbonyl groups are omitted for clarity), where the forward reactions of (k) to (m) are proposed for the reduction. These are obviously very similar to the forward reactions of (g) to

(10) Fukuzumi, S.; Ohkubo, K.; Tokuda, Y.; Suenobu, T. *J. Am. Chem. Soc.* **2000**, *122*, 4286.

(i), the only real difference being, in step (1) a dimer of **4** rather than an aggregate of **3** and **4** is proposed. As shown by (n), the oxidation of **2** to **3** by acid also follows a mechanism very similar to that of **1** to **2**. Here also the rate-determining step (*rds*) is preceded by a fast protonation equilibrium, but a single proton rather than two or three protons is involved in the equilibrium.

As already mentioned, apart from the empirical rate expression, indirect support for the proposed mechanism comes from a variety of sources. First, formation of dimers and aggregates of the clusters provides a simple mechanism for the intermolecular exchange of platinum triangles. As mentioned, such exchange had indeed been observed by ^{195}Pt NMR. The apparent negative activation energy is also consistent with thermodynamically favorable dimerization equilibrium. The reason that the dimer of **2** is not observed by spectrophotometry is probably because it is a weak van der Waals type aggregate, and only negligible electronic perturbation is caused by the aggregation or dimerization.

Second, it has recently been reported that when conventionally prepared platinum colloids are reacted with carbon monoxide, *aggregates* of the Chini clusters are formed.[11] Thus, aggregate formation by these carbonyl clusters seems to be thermodynamically feasible and favored. Third, several reversible one- and two-electron redox steps have been reported[9] in the cyclic voltammogram of $[Pt_{24}(CO)_{30}]^{n-}$ and $[Pt_{26}(CO)_{32}]^{n-}$ ($n = 0-10$). To a first approximation, this means that high nuclearity is a prerequisite for the ability to act as a reversible and facile electron sink. This observation is the rationale behind proposing that electron transfers require the involvement of trimers **1** and **2**.

Fourth, aggregation may be seen as an extrapolation of the donor and acceptor properties[12] of complexes of the general formula $Pt_3L_3(CO)_3$. Such donor and acceptor properties are expected to be amplified for $[Pt_3(CO)_6]^{2-}$ (donor) and $[Pt_3(CO)_6]$ (acceptor), with that of $[Pt_{3n}(CO)_{6n}]^{2-}$ clusters falling somewhere in between. Fifth, by liquid X-ray scattering a mixture of $[Ni_6(CO)_{12}]^{2-}$ and $[Pt_6(CO)_{12}]^{2-}$ in acetone has been shown to lead to the formation of $[Ni_6Pt_6(CO)_{21}]^{4-}$ presumably through dimerization followed by CO loss.[13] Finally the aggregation of platinum carbonyl clusters has also been seen in the gas phase by plasma desorption massspectrometry.[14]

Conclusion

The orders of the forward and backward reactions of equilibrium (d) are found to be first and second with respect to the concentrations of **1** and **2**, respectively. The forward reaction shows saturation kinetics and complex dependence on the acid concentration, indicating several protonation equilibria. The backward reaction rate is independent of the hydrogen pressure within the pressure range of 1−7 bar. The acid-induced oxidations of **2** to **3** in both DMF and acetonitrile proceed through fast protonation equilibria involving one proton followed by rate-determining steps. Cyclic voltammetric studies on **1** in DMF and **2** in acetonitrile show three and two anodic responses, respectively. In accordance with qualitative observations, the redox potentials indicate that oxidation is thermodynamically more favorable in acetonitrile than in DMF. A general mechanism is proposed for the backward reactions of equilibria (d) and (f). In a sequential manner this involves aggregation (dimerization) → disproportionation → aggregation (or dimerization) → disproportionation. Aggregates or trimers of **1** and **2** are proposed to be involved in the electron transfer steps of (d) and (f), respectively.

Experimental Section

All reactions and manipulations were carried out under an atmosphere of dry nitrogen or argon unless stated otherwise. The platinum clusters **1**−**4** were prepared according to literature-reported procedure.[2] Infrared spectra were recorded using a Perkin Elmer 781 spectrophotometer. Cyclic voltammetric measurements were carried out under an atmosphere of dry nitrogen or argon using a Princeton Applied Research instrument. A platinum working electrode, a platinum-wire auxiliary electrode, and an aqueous saturated calomel reference electrode (SCE) were used in a three-electrode configuration. $(Bu)_4N^+BF_4^-$ was used as supporting electrolyte. The UV−vis spectra and kinetic monitoring were performed on a Shimadzu UV-160 instrument.

Kinetic Studies. The mathematical techniques for the simulation studies have been reported earlier[15] and are available as Supporting Information. Reduction of **2** to **1** by dihydrogen at atmospheric pressure was carried out in an ordinary cell equipped with a rubber septum or in a special cell purchased from Hellma GmbH. Preliminary experiments at atmospheric pressure of dihydrogen showed dependence of rate on the rate of agitation or bubbling of the gas. This indicated that macroscopic mass transfer effects were important. The rate studies at atmospheric pressure of dihydrogen were therefore carried out under a constant rate of the gas flow.

A known quantity of **2** was dissolved in dihydrogen-saturated DMF, a constant hydrogen flow was maintained, and the UV−vis spectra were recorded at regular time intervals. Experiments under constant elevated pressures of dihydrogen were carried out in small glass vessels contained in a 100 mL Parr pressure reactor and by measuring the initial rates. The solubility data of dihydrogen in DMF and acetonitrile are available in the literature.[16] For the kinetic runs under atmospheric pressure, concentration of the cluster in DMF was maintained at 10^{-5} M L^{-1} level.

The Arrhenius plot was based on four different runs at each of four different temperatures. As the temperature is raised, the solubility of dihydrogen in DMF is expected to decrease. Assuming ideal gas behavior under these conditions, the rate constant $k = (A/T)e^{-\Delta E/RT}$. Thus, $\ln(kT)$ versus $1/T$ was also plotted, but the difference between this and the conventional Arrhenius plot, $\ln(k)$ versus $1/T$, was found to be negligible.

The oxidation of **1** by acid was initiated by adding a given quantity of aqueous perchloric acid of known strength to a DMF solution of **1** maintained at a constant temperature in the UV cell. In a few experiments aqueous hydrochloric acid was used in place of aqueous perchloric acid. Several control experiments established that there was no noticeable difference between the two sets of data using the two different acids.

(11) Henglein, F. A. *J. Phys. Chem. B* **1997**, *101*, 5889.
(12) Venanzi, L. M.; Imhof, D. *Chem. Soc. Rev.* **1994**, *23*, 185.
(13) Bengtsson-Kloo, L.; Iapalucci, C. M.; Longoni, G.; Ulvenlund, S. *Inorg. Chem.* **1998**, *37*, 4335.
(14) Mcneal, C. J.; Huges, J. M.; Lewis, G. J.; Dahl, L. F. *J. Am. Chem. Soc.* **1991**, *113*, 372.
(15) (a) Bhaduri, S.; Sharma, K.; Mukesh, D. *J. Chem. Soc., Dalton Trans.* **1993**, 1191. (b) Bhaduri, S.; Sharma, K.; Mukesh, D.; *J. Chem. Soc., Dalton Trans.* **1992**, 77. (c) Norris, A. C. *Computational Chemistry−An Introduction to Numerical Methods*; Wiley: New York; 1981.
(16) Brunner, E. *J. Chem. Eng. Data* **1985**, *30*, 269.

The concentrations of **1**, **2**, and **3** were within the range where Beer−Lambert's law was valid. This was verified by separate calibration curves for **1**−**3**.

Acknowledgment. Financial support received from the Department of Science and Technology, New Delhi, India, is gratefully acknowledged. The referees' suggestions at the revision stage were very helpful.

Supporting Information Available: This material is available free of charge via the Internet at http://pubs.acs.org.

OM0102201